International Journal of Theoretical Physics, Vol. 17, No. 3 (1978), pp. 189–199

Wave Optics of the Spherical Gravitational Lens. II. Diffraction of a Plane Electromagnetic Wave by a Black Hole

E. Herlt and H. Stephani

Wissenschaftsbereich Relativistische Physik, Sektion Physik, Friedrich-Schiller-Universität Jena, DDR-69 Jena, Max-Wien-Platz 1

Received January 20, 1977

This paper gives (in a suitable approximation) the Poynting vector of a plane electromagnetic wave diffracted by the gravitational field of a Schwarzschild black hole. The relation between the approximation procedure and the concept of rays is established. The main results are as follows: (1) On the focal line an extreme amplification of intensity takes place. (2) In the whole space off this focal line a double image is to be seen. (3) Rays having revolved around the black hole repeatedly give small corrections only. (4) The phase differences (transit-time differences) along the different rays are computed.

1. INTRODUCTION

In a preceding paper (Herlt and Stephani, 1976), from now on referred to as I, we discussed in detail the gravitational lens effect of a star large compared to its Schwarzschild radius. Here we shall deal with the image of a very distant star produced by a black hole. The main difference from the large star case is that, in the field of a black hole, interference can take place in the whole space (there is no shadow), and that, owing to rays that repeatedly revolve around the center, ghost images may appear.

We start with a short account of formulas derived in I, which enable us to give the components of the Poynting vector in terms of the Debye potential P and to evaluate P by the method of stationary phase. The connection between this method and the concept of rays is discussed in Sections 3 and 4.

0020–7748/78/0300–0189$05.00/0

In Section 5 the shape of the image due to the two main rays is given, and in Section 6 the corrections due to the secondary rays (rays having revolved around the black hole several times) are discussed. Section 7 deals with the transit-time differences along the different rays. We finish with some remarks on possible observations.

2. NOTATIONS AND GENERAL EXPRESSION FOR THE POYNTING VECTOR OF THE DIFFRACTED WAVE

As shown in I, the electromagnetic field in a Schwarzschild background that corresponds to an incident plane wave can be given in terms of the function P:

$$P(r, \vartheta) = \sum_{n=1}^{\infty} \frac{(-1)^n(2n+1)}{2\omega^2 n(n+1)} e^{i\omega(1/2 - \ln 2)}[R_n^{\text{in}}(r) + R_n^{\text{out}}(r)]P_n^1(\cos\vartheta) \tag{2.1}$$

Here the P_n^1 are the Legendre functions, the $R_n(r)$ are solutions of the radial equation

$$\frac{d^2R}{dv^2} + \omega^2\left[1 - a^2\frac{r-1}{r^3}\right]R_n = 0 \tag{2.2}$$

$$v \equiv r + \ln(r-1), \qquad a^2 \equiv n(n+1)/\omega^2$$

ω is the frequency of the wave, and r and ϑ are spherical coordinates chosen as in Figure 1. All distances are measured in units of the Schwarzschild radius; so the horizon is at $r = 1$, and ω is 2π times the Schwarzschild radius divided by the (flat space) wave length.

From now on we confine attention to the physically most interesting case $\omega \gg 1$ ($\omega = 10^{10}$ for visible light and a black hole of about one solar mass)

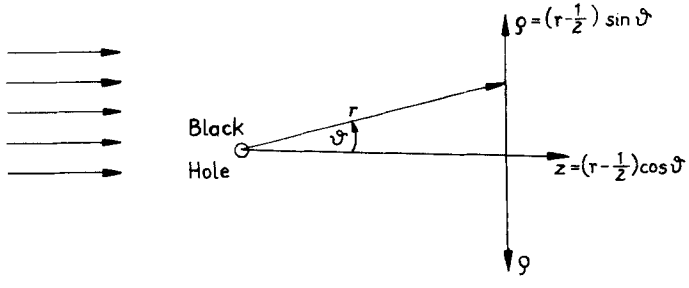

Fig. 1. Coordinate systems.

and $r \gg 1$ (observer on earth, far away from the nearest black hole). We then can use the WKB method to approximate the radial functions by

$$R_n^{\text{in}}(r) = \frac{e^{-i\omega(v+T)}}{[1 - a^2(r-1)/r^3]^{1/4}}$$
$$R_n^{\text{out}}(r) = \frac{e^{i\omega(v+T-W)}}{[1 - a^2(r-1)/r^3]^{1/4}} \tag{2.3}$$

R_n^{out} being zero for $a^2 < 27/4$, with

$$T(r, n) = \int_r^\infty \left[1 - \left(1 - a^2 \frac{r-1}{r^3}\right)^{1/2}\right] \frac{r}{r-1}\, dr$$
$$\approx a \arcsin(a/r) + (1 - a^2/r^2)^{1/2} - r + 1$$
$$- \ln 2 + \ln[1 + (1 - a^2/r^2)^{1/2}] \tag{2.4}$$

and

$$W(n) = 2\int_{r_0}^\infty \left[1 - \left(1 - a^2 \frac{r-1}{r^3}\right)^{1/2}\right] \frac{r}{r-1}\, dr$$
$$+ 2r_0 + 2\ln(r_0 - 1) - \frac{\pi}{2\omega} \tag{2.5}$$

$$\frac{r_0^3}{r_0 - 1} \equiv a^2$$

Taking the well-known asymptotic representation of the Legendre functions and neglecting the R_n^{in}, which would contribute only for $\pi/2 \leqslant \vartheta \leqslant \pi$, we finally obtain

$$P(r, \vartheta) = -\sum_{n + 1/2 = (w/2)3(3)^{1/2}}^{\infty} \frac{e^{i\omega(1/2 - \ln 2)}}{\omega^2(2\pi n \sin\vartheta)^{1/2}} \frac{e^{i\omega(v+T-W)}}{[1 - a^2(r-1)/r^3]^{1/4}} \cdot e^{in\cdot 2m\pi}$$
$$\times \{e^{i[(n+1/2)\vartheta - 3\pi/4]} - e^{-i[(n+1/2)\vartheta - 3\pi/4]}\} \tag{2.6}$$

where m is an arbitrary integer.

From (2.6) we can get the components of the Poynting vector by computing

$$\alpha = -\sin\vartheta \frac{\partial}{\partial\vartheta} \frac{1}{\sin\vartheta} \frac{\partial}{\partial\vartheta} (\sin\vartheta P)$$
$$\beta = \sin\vartheta \frac{\partial}{\partial\vartheta} \frac{\partial}{\partial v} P + i\omega P \tag{2.7}$$
$$\delta = -i\omega \sin\vartheta \frac{\partial P}{\partial\vartheta} - \frac{\partial P}{\partial v}$$

and substituting the result into

$$S_z = -\frac{1}{r^2 \sin\vartheta} \operatorname{Re}(\delta e^{-i\omega t}) \operatorname{Re}\left\{\left[\frac{\alpha}{r^2}(r - \tfrac{1}{2}) + \beta \operatorname{cotan}\vartheta\right] e^{-i\omega t}\right\}$$
$$S_\rho = \frac{1}{r^2 \sin\vartheta} \operatorname{Re}(\delta e^{-i\omega t}) \operatorname{Re}\left\{\left[\frac{\alpha}{r^2}(r - \tfrac{1}{2}) \operatorname{cotan}\vartheta - \beta\right] e^{-i\omega t}\right\} \tag{2.8}$$

The equations (2.6)–(2.8) are valid for $\omega \gg 1, r \gg 1, n \sin\vartheta \gg 1, \vartheta < \pi/2$. On the axis $\vartheta = 0$ similar results can be obtained.

3. METHOD OF STATIONARY PHASE AND RAYS

As in I, we evaluate the infinite sum (2.6) by replacing it by an integral over n and using the method of stationary phase. The points $n = n_0$ of stationary phase are obviously given by

$$\frac{\partial S}{\partial n} = \frac{\partial}{\partial n}(\omega T - \omega W + n\pi \pm n\vartheta + n2m\pi) = 0 \tag{3.1}$$

This equation admits a simple interpretation in terms of geometrical optics. Because of (3.1) the lines $n_0 = n_0(r, \vartheta) = \text{const}$ fulfil

$$\pm d\vartheta + \omega \frac{\partial^2 T}{\partial r \partial n} dr = 0 \tag{3.2}$$

or, taking the definition (2.4) of $T(r, n)$,

$$\left(\frac{dr}{\partial\vartheta}\right)^2 = \frac{r^4}{a^2} - r(r - 1) \tag{3.3}$$

On the other hand, the first integrals of the null geodesics equation in the Schwarzschild metric are

$$r^2 \frac{d\vartheta}{d\lambda} = B, \qquad \frac{r-1}{r}\frac{dt}{d\lambda} = A,$$
$$\frac{r-1}{r}\left(\frac{dr}{d\lambda}\right)^2 + r^2\left(\frac{d\vartheta}{d\lambda}\right)^2 - \frac{r-1}{r}\left(\frac{dt}{d\lambda}\right)^2 = 0 \tag{3.4}$$

which yield

$$\left(\frac{dr}{d\vartheta}\right)^2 = \frac{A^2}{B^2} r^4 - r(r - 1) \tag{3.5}$$

If we identify B^2/A^2 with a^2, equations (3.3) and (3.5) coincide. So we can state that the lines connecting points of stationary phase of equal n_0 are exactly the rays of geometrical optics. There are exactly as many points of stationary phase that contribute to the wave field in a given point (r, ϑ) as

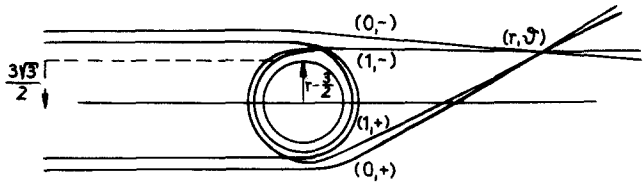

Fig. 2. The different types $(m, \pm)$ of rays outside a black hole.

there are rays crossing this point. Moreover, the equivalence of (3.3) and (3.5) shows that the approximation procedure of this paper is closely related to the usual short-wavelength approximation of wave optics. In the case of the Schwarzschild background it is well known that for an incident plane wave (parallel rays for $r \to \infty$, $\vartheta = \pi$) each point (r, ϑ) is passed by an infinite number of rays. These rays differ (see Figure 2) in their sense of revolution (indicated by $\pm$) and the number $m \geqslant 0$ of revolutions they have performed. Using the same notation to label the points of stationary phase, we obtain from (2.6)

$$P(r, \vartheta) = -\frac{e^{i\omega(1/2 - \ln 2)} e^{-i\pi/4}}{\omega^2 (\sin \vartheta)^{1/2}} \times \sum_{m=0}^{\infty} \left\{ \frac{e^{iS(m,-)}}{[1 - a^2(m,+)(r-1)/r^3]^{1/4} [n_0(m,+) S''(m,+)]^{1/2}} - \frac{e^{iS(m,-)}}{[1 - a^2(m,-)(r-1)/r^3]^{1/4} [n_0(m,-) S''(m,-)]^{1/2}} \right\} \tag{3.6}$$

where

$$S(m, \pm) = \omega T[r, n_0(m, \pm)] - \omega W[n_0(m, \pm)] \pm [n_0(m, \pm) + \tfrac{1}{2}][\vartheta \pm 2m\pi] + \omega v + [n_0(m, \pm) - m]\pi \mp \pi/4 \tag{3.7}$$

$n_0(m, \pm)$ are the solutions of (3.1), and S'' is the second derivation of S with respect to n.

The derivatives of P that we need to get α, β, and δ can be calculated (at least off the axis $\vartheta = 0$) simply by taking the derivatives of the factors $e^{iS(m,\pm)}$, because only these derivatives contain a factor ω. From (2.6) and (3.1) one gets

$$\frac{\partial}{\partial v} e^{iS(m,\pm)} = i\omega \left[1 - a^2(m, \pm) \frac{r-1}{r^3}\right]^{1/2} e^{iS(m,\pm)}$$
$$\frac{\partial}{\partial \vartheta} e^{iS(m,\pm)} = \pm i\omega a(m, \pm) e^{iS(m,\pm)} \tag{3.8}$$

4. NUMBER OF RAYS

At first glance the change from (2.6) to (3.6) seems to be a rather doubtful success: We again have to deal with an infinite sum involving complicated functions. But a careful analysis shows that the contributions with large m are negligible.

Because of (3.1) large values of m correspond to large values of

$$\omega \frac{\partial W}{\partial n} = 2\int_{r_0}^{\infty} \frac{a\,dr}{[r^4 - a^2 r(r-1)]^{1/2}}, \qquad r_0{}^3/r_0 - 1 \equiv a^2 \tag{4.1}$$

that is to values of r_0 close to 3/2, where the quadric $r^4 - a^2 r(r-1)$ has a double zero. In this region the elliptic integral (4.1) can be approximated by

$$\begin{aligned} \omega \frac{\partial W}{\partial n} &= -4 \ln \frac{1+\sqrt{3}}{6} - 2 \ln (r_0 - \tfrac{3}{2}) + \tfrac{16}{9}(r_0 - \tfrac{3}{2}) + \cdots \\ \frac{n+\frac{1}{2}}{\omega} &= a = \frac{3\sqrt{3}}{2}\,[1 + \tfrac{2}{3}(r_0 - \tfrac{3}{2})^2 - \cdots] \end{aligned} \tag{4.2}$$

Substituting (4.2) into (3.1) and neglecting $\omega(\partial T/\partial n)$ (which is of order r^{-1}), the points of stationary phase with $m > 1$ are given by

$$\tfrac{1}{2} + n_0(m, \pm) \approx \frac{\omega 3\sqrt{3}}{2}\left[1 + \frac{2}{3}\frac{18^2}{(2+\sqrt{3})^2}\, e^{-(2m+1)\pi \pm \vartheta} + \cdots\right] \tag{4.3}$$

For large m these points accumulate near $n_0(\infty, \pm) = (\omega 3\sqrt{3} - 1)/2$. Now we have to remember that originally n was a discrete integral variable. Replacing this discrete variable by a continuous one and using the method of stationary phase makes sense only if n is large and, what is more important in this context, if the points of stationary phase are separated from each other by distances large compared to unity. Accordingly, we have to limit m to those values that ensure $n_0 + 1/2 \geqslant \omega 3\sqrt{3}/2 + 1$, that is to

$$m \leqslant \ln \omega/2\pi + 0.09 \tag{4.4}$$

To take into account contributions with larger m would mean to take terms comparable in magnitude to those already neglected by the very use of the WKB approximation and the method of stationary phase. The meaning of the limitation (4.4) is that the concept of rays is applicable only as far as neighboring rays have a distance larger than the wavelength.

5. IMAGE OF A STAR DUE TO THE MAIN RAYS (0, −) AND (0, +)

As will be shown later, the shape of a star's image is mainly determined by the two rays (0, −) and (0, +), i.e., by the interference pattern of the two associated waves.

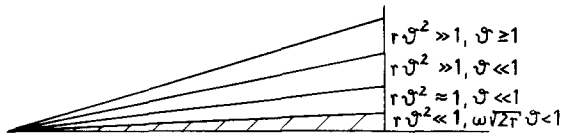

Fig. 3. Regions with different character of a star's image.

For $\vartheta \ll 1$ these two rays pass the black hole at a very large distance; therefore, the calculations of I are applicable in that case. The main results listed there are (see Figure 3) as follows.

(1) For $r\vartheta^2 \ll 1$ there is a focal beam of extreme intensity. Its diameter is about $2(r\lambda/\pi)^{1/2}$, and the magnitude of the Poynting vector is enlarged up to a factor $\pi\omega$. An observer located in this focal beam will see an undeflected bright star.

(2) For $r\vartheta^2 \approx 1$ an observer will see a double image of unequal brightness, the undeflected part being the brighter one.

(3) For $r\vartheta^2 \gg 1$, $\vartheta \ll 1$ the observer will see a double image of equal brightness. As in (2), the deflection angle is $\Delta_2 = -S_\rho/S_z = 4/r\vartheta$, the peak at $\Delta_1 \approx 0$ being nearly undeflected.

We now will deal with the region $r\vartheta^2 \gg 1$, $0.01 \leqslant \vartheta \leqslant \pi/2$. Here the assumption that the star is a black hole is essential, because the ray $(0, +)$ would be absorbed at the surface of the star. For the two main rays we get from (3.1) and (2.4)–(2.5)

$$a(0, -) = r \sin\vartheta\left[1 + \frac{(1 + \cos\vartheta)^2}{2r \sin^2\vartheta}\right]$$
$$S''(0, -) = 1/\omega r \cos\vartheta \tag{5.1}$$

and

$$\vartheta \approx 2\int_{r_0(0,+)}^{\infty} \frac{a(0, +)\, dr}{[r^4 - a^2(0, +)r(r - 1)]^{1/2}} - \pi$$
$$S''(0, +) = -\frac{2}{\omega}\frac{\partial}{\partial a(0, +)}\int_{r_0(0,+)}^{\infty} \frac{a(0, +)\, dr}{[r^4 - a^2(0, +)r(r - 1)]^{1/2}} \tag{5.2}$$

No simple approximation of these elliptic integrals is available for $\vartheta \approx 1$; we have to evaluate them numerically to get $a(0, +)$ and $S''(0, +)$ in terms of ϑ.

The time-averaged components of the Poynting vector prove to be

$$\bar{S}_z = \tfrac{1}{2}$$
$$\bar{S}_\rho = -\frac{1}{2r}\left\{\frac{1 + \cos\vartheta}{\sin\vartheta} + \left[\frac{a(0, +)\sin\vartheta}{\omega S''(0, +)}\right]^{1/2} \cos\left[S(0, -) - S(0, +)\right]\right\} \tag{5.3}$$

TABLE I. The deflection angles Δ_1 and Δ_2 as functions of r and ϑ

r_0	ϑ	$r\Delta_1$	$r\Delta_2$
$r_0 \gg 1$	$2/r_0$	-0.74	$4/\vartheta = 2r_0$
16.77	7.27°	-0.74	32.33
8.248	15.79°	-0.695	15.12
4.090	37.20°	-0.596	6.558
2.786	65.49°	-0.498	4.608

Because of

$$\frac{\partial}{\partial\rho}[S(0,-) - S(0,+)] \approx \frac{\partial}{\partial\rho}[S(0,-) - S(m,\pm)] \approx -\omega\sin\vartheta \tag{5.4}$$

the deflection angle $\Delta = -\arctan \bar{S}/\bar{S}_z = -2\bar{S}_\rho$ oscillates rapidly over the aperture of a telescope, and therefore the image of the star is determined essentially by the angular distribution $dI/d\Delta$ of the intensity I. From (5.3) we get

$$\frac{dI}{d\Delta} = \frac{r\sin\vartheta}{4}\left|\left(\frac{dS_\rho}{\partial\rho}\right)^{-1}\right| d\psi \approx \frac{r\,d\psi}{2\omega}\cdot\frac{1}{\sqrt{(\Delta_2 - \Delta)(\Delta - \Delta_1)}} \tag{5.5}$$

with

$$\begin{aligned}\Delta_2 - \Delta_1 &= \frac{2}{r}\sqrt{\frac{a(0,+)\sin\vartheta}{\omega S''(0,+)}}\\ \Delta_1 + \Delta_2 &= \frac{2}{r}\frac{1+\cos\vartheta}{\sin\vartheta}\end{aligned} \tag{5.6}$$

Some values of $\Delta_2 \pm \Delta_1$ are given in Table I. According to (5.5), an observer will see a double image of equal brightness, i.e., two peaks of (equal) intensity at Δ_1 and Δ_2 and a weak bridge in between (see Figure 4). This result differs considerably from geometrical optics, which predicts a main image at $(\Delta_1 + \Delta_2)/2$ and a weak secondary image (intensity $\sim r^{-2}$) at $\Delta = -\vartheta$.

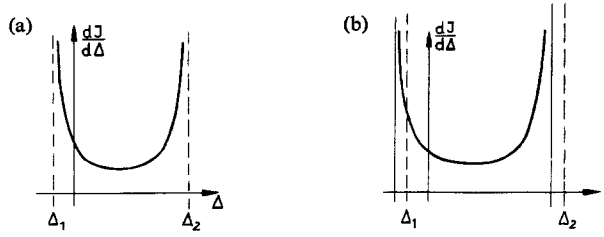

Fig. 4. Image of a star in the region $r\vartheta^2 \gg 1$. (a) Main rays only; (b) main + secondary rays.

6. CONTRIBUTIONS FROM THE SECONDARY RAYS $(m, \pm)$, $m \geq 1$

As already mentioned in Section 4, for $m \geqslant 1$ the points of stationary phase and the phase and its second derivative at these points are approximately given by

$$\begin{aligned} n_0(m, \pm) + \tfrac{1}{2} &\approx \frac{\omega 3\sqrt{3}}{2}\left[1 + \frac{2}{3}\cdot\frac{18^2}{(2+\sqrt{3})^2}\, e^{-(2m+1)\pi \pm \vartheta}\right] \\ S(m, \pm) &\approx \frac{\omega 3\sqrt{3}}{2}[(2m+1)\pi \pm \vartheta] - m\pi + \omega r \\ &\quad + \omega \ln r + \text{const} \\ \omega S''(m, \pm) &\approx \frac{1}{\sqrt{3}}\,\frac{(2+\sqrt{3})^2}{18^2}\, e^{(2m+1)\pi \pm \vartheta} \end{aligned} \tag{6.1}$$

We see that the main m-dependent part of the phase $S(m, \pm)$ originates from the revolution in the circle $r = 3/2$, which has the optical path length $3\sqrt{3}\pi$.

If we put (6.1) into the machinery of the formulas (2.7), (2.8), (3.6), and (3.8) and work it out, we find the following.

(1) In (3.6) the amplitudes attached to the rays $(m, \pm)$ are smaller than those attached to $(0, -)$ by a factor of order r^{-1} and smaller than the amplitudes of $(0, +)$ at least by a factor $e^{-\pi} \approx 0.04$.

(2) The amplitudes of two successive rays $(m, \pm)$ and $(m+1, \pm)$ decrease by a factor $e^{-\pi}$. The contributions of a ray with $m = \ln \omega/2\pi$ are, therefore, of order $1/\sqrt{\omega}$ and can be neglected. This supports the reasoning of Section 4, where we limited the number of rays.

(3) If there is an important contribution of the secondary rays to the Poynting vector at all, it should be in the region $r\vartheta^2 \gg 1$. Here

$$\begin{aligned} \bar{S}_z &= \tfrac{1}{2} \\ \bar{S}_\rho &= -\frac{1}{2r}\left\{\frac{1+\cos\vartheta}{\sin\vartheta} + \left[\frac{a(0,+)\sin\vartheta}{\omega S''(0,+)}\right]^{1/2}\cos[S(0,-) - S(0,+)]\right. \\ &\quad + \sum_{m=1} 2.85 e^{-m\pi}(\sin\vartheta)^{1/2}(e^{-\vartheta/2}\cos[S(0,-) - S(m,+)] \\ &\quad \left. + e^{-\vartheta/2}\cos[S(0,-) - S(m,-)])\right\} \end{aligned} \tag{6.2}$$

holds; compare Section 5. Since the coefficients of $\cos[S(0,-) - S(m,\pm)]$ are small compared to $[a(0,+)\sin\vartheta/S''(0,+)]^{1/2}$, the zeros of $\partial\bar{S}\rho/\partial\rho$ and the corresponding peaks of intensity are both in the neighborhood of Δ_1 and Δ_2, and no further peaks appear. The image of the star would only change

from that of Figure 4a to that of Figure 4b. The smaller ϑ becomes, the smaller are the changes to be expected.

(4) On the axis $\vartheta = 0$ the secondary rays, too, will give a diffraction peak (amplification of intensity by a factor $\pi\omega$), which is broader than the main peak by a factor $\sqrt{r}$. Nevertheless, this peak is negligible, because the image is dominated by the much brighter main peak.

To summarize, the secondary rays for an incident coherent plane wave nowhere give an essential contribution.

7. INCOHERENT SUPERPOSITION OF RAYS

The various rays $(m, \pm)$ have rather different optical path lengths. The differences of their phases $S(m, \pm)$ are, in detail,

$$
\begin{aligned}
&S(0,+) - S(0,-) \approx 2\omega(2r)^{1/2}\vartheta \qquad \text{if } r\vartheta^2 \ll 1\\
&S(0,+) - S(0,-) \approx \omega r\vartheta^2/2 + \omega 2 \ln r\vartheta^2 \qquad \text{if } r\vartheta^2 \gg 1,\ \vartheta \ll 1\\
&S(m,+) - S(m,-) \approx \omega 3\sqrt{3}\vartheta\\
&S(m,+) - S(\bar{m},+) \approx \omega 3\sqrt{3}\pi(m - \bar{m}) \qquad (7.1)\\
&S(m,\pm) - S(0,-) = \omega\{r(1 - \cos\vartheta) + \ln 8r^2 \sin^2\vartheta/(1 + \cos\vartheta) + \cos\vartheta\\
&\qquad + 3 - 6\ln(2 + \sqrt{3}) - \pi/2 + 3\sqrt{3}\\
&\qquad \times [(m + \tfrac{1}{2})\pi \pm \vartheta/2 - 1]\} \qquad \text{if } r\vartheta^2 \gg 1\\
&S(m,\pm) - S(0,-) = \omega[\ln 16r + 3 - 6\ln(2 + \sqrt{3}) - \pi/2\\
&\qquad + 3\sqrt{3}\{(m + \tfrac{1}{2})\pi \pm \vartheta - 1\}] \qquad \text{if } r\vartheta^2 \ll 1
\end{aligned}
$$

As all distances are measured in units of the Schwarzschild radius, a phase difference ω corresponds to a path difference of one Schwarzschild radius, which for a typical star is of order 1 km.

If the coherence distance is smaller than the path differences listed above, geometrical optics is applicable. It can easily be shown that in this case (superposition of intensities instead of amplitudes) the results of the approximation procedure presented here fully agree with those of geometrical optics. Near the axis $\vartheta = 0$ rays of equal m always have small path differences, they are coherent, and they give the typical diffraction peak at the focal line.

If the source emits pulses of light, pulses being propagated along different rays suffer a transit-time difference according to the phase differences (7.1).

8. OBSERVATIONAL CONSEQUENCES

In I we have already discussed the image of a large star. We therefore will restrict ourselves to the question of whether there is a possibility of

distinguishing a large star from a neutron star or a black hole by means of the image it produces.

As we have shown, in the case of a coherent incident wave the secondary rays give negligible contributions only. The shape of the image is determined by the main rays, and off the axis $\vartheta = 0$ a double image is to be seen. But the very fact that an observer sees a double image may contain useful information, because a double image can be formed only if the ray $(0, +)$ is not absorbed at the surface of the star in question. If at a point (r, ϑ) a double image is detected, we can use (5.1) or Table I to find the corresponding value of $a(0, +) = r_0(r_0/r_0 - 1)^{1/2}$ and conclude that the (coordinate) radius of the star is smaller than r_0.

If the source emits pulses of light, conclusions can be drawn similarly from the existence or nonexistence of the echoes due to the rays $(0, +)$ and $(m, \pm)$. The time delay of these echoes can be evaluated, too. The probability of detecting the echoes from the secondary rays is rather small, because their intensity is smaller than that of the main signal by a factor

$$\frac{a(m, \pm)}{S''(m, \pm) r^2 \sin \vartheta} \approx \frac{0.004 e^{-[(2m+1)\pi \pm \vartheta]}}{r^2 \sin \vartheta}$$

for $r\vartheta^2 \gg 1$ and

$$7.2 \times 10^5 e^{-(2m+1)\pi}/r^2$$

for $\vartheta \approx 0$.

REFERENCES

Darwin, C. (1959). *Proceedings of the Royal Society*, **249**, 187.
Herlt, E., and Stephani, H. (1976). *International Journal of Theoretical Physics*, **15**, 45.